XLI CILAMCE
XLI Ibero-Latin American Congress on Computational Methods in Engineering
16-19 November, 2020 FOZ DO IGUAÇU PARANÁ – BRAZIL

H-FEM AND FSDT TO APPROACH THE FREE AND FORCED VIBRATION OF A GRAPHENE SHEET USING A NON-LOCAL CONTINUUM MECHANICS THEORY

Oscar A. Garcia[1], Rodrigo Rossi[1]

[1]*Depto. de Engenharia Mecânica, Universidade Federal do Rio Grande do Sul*
Sarmento Leite 425, 90050-070, Porto Alegre/RS, Brazil
oagsuarez@gmail.com, rossi@ufrgs.br

Abstract. The allotropic forms of carbon as nano tubes and more recently graphene sheet has gained significant notoriety in the last two decades where its use has been spread in the most diverse areas such as composite materials, electronics, medicine, fine chemistry, among others. Within this context, the mechanical behavior of wave propagation at the nanoscale level has received special attention for its relevance in the application of transport problems of molecules, sensors for detecting gas atoms, resonators for high frequencies, among others. Recently, classical approaches to nanoscale problems with atomic and hybrid models, more accurate but with high computational cost, have left some room for approaches that use the principles of continuum mechanics with the classic (local) and non-local versions. The results observed in the literature on free vibration problems, obtained with non-local continuous mechanics, have been closer to the results of molecular dynamics than those obtained with classical or local continuous mechanics. In this work, the authors propose an approach using the non-local continuum mechanics for the free and forced vibrations problems in graphene sheets using the approximation spaces obtained with Hermite finite elements (H-FEM) with regularity $C^k(\Omega), k = 1,2$ together with the first order plate model "First Shear Deformation Theory" (FSDT). This approach intends to investigate some aspects of the analyzed problem to improve the proximity of the response to that obtained using molecular dynamics: provide the regularity requirements of the non-local model equilibrium equations; improve accuracy in natural modes and frequencies using highly regular approximation spaces; improve the accuracy of the response of natural modes and frequencies by incorporating the rotational inertia introduced by the kinematic FSDT model.

1 Introduction

The use of carbon allotropic forms such as the nanostructures of fullerene tubular arrangements and graphene sheets has gained centrality in the development of nano technology due to the superior mechanical properties shown by the high modulus of elasticity (Y. Nan and L. Vicenzo, [1]) and super thermal and electrical conductivity (A. Moisala et al., [2]). Within this context, the simulation of the dynamic behavior of nano structures has been a subject of recent research, in which atomic methods are used, including molecular dynamics (MD) (S.C. Chowdhury et al., [4]); tight binding molecular dynamic (TBMD) and the density functional theory (DFT), (D. Sanchez-Portal et al., [5]). The methods are accurate but require a high computational time, which makes their use limited to a small number of molecules involved in the model. An alternative, with a lower computational cost, was proposed using the mechanics of the non-local continuum by A. C. Eringen [6] and [7] where the state of stresses at a point depends on the state of deformations in its neighborhood. In this context, the applications of this theory in free vibrations have been studied by several authors. R. Ansari et al. [8] studied simple sheets of graphene using the first order plate model with shear strain (FSDT) and the Generalized Differential Quadrature Method (GDQM). L. W. Zhang., et al. [9] studied nonlinear vibration problems of nanoplates using classical lamination theory (CLT) and the k-Rittz method. On the other hand, in problems of propagation and dispersion of mechanical waves in nanoplates, of fundamental importance in the design of large molecule dispersers and gas sensors, stand out the studies of B. Arash et al., [10] that simulate nano sensors using thin plate models together with Hermite finite elements. T. Aksencer and M Aydogdu [11] study the effects of nanoscale coefficients, dimensions, and boundary conditions on the propagation and dispersion of mechanical waves on thin nano plates using analytical

solutions. Mohammad R. B. and S. Hossein [12] use Strain Gradient's non-local theory and Galerkin's method to study the effects of mechanical wave dispersion on resonance in porous material nanoplates in functional gradients modeled with high-order kinematic theories. In this work, the authors address the problem of free and forced vibrations in simply supported nanoplates with kinematic theory modeled by FSDT. The elastodynamic equations at the nanoscale are obtained considering the principles of non-local elasticity of [7]. The approximation space is built with finite elements of Hermite (R. Mazzochi, [13]) of high regularity and high order, to avoid shear locking and improve the responses to eigenvalues/eigenvectors problems in the free vibration version. The results for the first frequency are compared with those obtained by [8] and those for mechanical wave propagation are analyzed with respect to a reference solution obtained using the bi-harmonics functions for FSDT plates according to J. N. Reddy, [14].

2 Non-local elastodynamics

In this section, dynamic equilibrium equations are briefly introduced, incorporating non-local elasticity in Mindlin plates (FSDT) and the semi-discrete formulation for the forced vibration problem.

2.1 Principles of non-local elasticity

One of the limitations of using classical or local continuum mechanics in nanoscale problems is the influence of the neighborhood that becomes significant in the responses of the state of stresses in a point $\boldsymbol{x}$ of the analyzed body. The study in [7] established a relation, shown in eq. (1), between the local stress tensor with sub index *l* and non-local with sub index *nl.* This equation can also be described by replacing $\boldsymbol{\sigma}_l\left(\boldsymbol{x}\right)$ by the constitutive equation of linear elasticity.

$$\left(1-\mu\nabla^2\right)\boldsymbol{\sigma}_{nl}\left(\boldsymbol{x}\right)=\boldsymbol{\sigma}_l\left(\boldsymbol{x}\right) \tag{1}$$

2.2 Non-local dynamic equilibrium equations

The non-local dynamic equilibrium equations for the thick plate element, shown in Fig.1 (a), of homogeneous and isotropic material are described in tensor form of internal forces in equations (3) to (10). In these equations, $\boldsymbol{N}$, $\boldsymbol{M}$ and $\boldsymbol{Q}$ are the normal force tensor, the bending moment tensor and shear force vector respectively. On the other hand, $\ddot{\boldsymbol{u}}$, $\ddot{\boldsymbol{\psi}}$ and $\ddot{\boldsymbol{w}}$ are the acceleration vectors of displacement in the middle plane, the acceleration vector of the rotations in the *x* and *y* directions (see, Fig.1(a)) and the acceleration of the transverse displacement. The terms I_j, *j=0,1,2*, are the coefficients of inertia described by

$$I_j=\int_{-h/2}^{h/2}z^j\rho\,dz.. \tag{2}$$

In equations (3) to (5) I_1 will be null if the material is homogeneous and isotropic. On the other hand, in equations (6) to (8), $\boldsymbol{N}_n$, $\boldsymbol{M}_n$ and Q_n are the vectors of normal force, bending moment and shear force on the boundary with normal $\boldsymbol{n}$ shown in Fig.1 (a).

Dynamic equilibrium equations for points $\left(x,y,0\right)\in\Omega$:

$$\nabla\cdot\boldsymbol{N}=\left(1-\mu\nabla^2\right)\left(I_o\ddot{\boldsymbol{u}}+I_1\ddot{\boldsymbol{\psi}}\right) \tag{3}$$

$$\nabla\cdot\boldsymbol{M}-\boldsymbol{Q}=\left(1-\mu\nabla^2\right)\left(I_1\ddot{\boldsymbol{u}}+I_2\ddot{\boldsymbol{\psi}}\right) \tag{4}$$

$$\nabla\cdot\boldsymbol{Q}=\left(1-\mu\nabla^2\right)\left(I_o\ddot{\boldsymbol{w}}-q\right) \tag{5}$$

Equilibrium equations for a point $\left(x,y,0\right)\in\Gamma_N$:

$$\boldsymbol{N} \cdot \boldsymbol{n} = \boldsymbol{N}_n \tag{6}$$

$$\boldsymbol{M} \cdot \boldsymbol{n} = \boldsymbol{M}_n \tag{7}$$

$$\boldsymbol{Q} \cdot \boldsymbol{n} = Q_n \tag{8}$$

$$\boldsymbol{u}\left(x, y, t_i\right) = \boldsymbol{u}^0\left(x, y\right), \ \ \forall\left(x, y\right) \in \Omega, \ t_i \in \left(0, T\right] \tag{9}$$

$$\dot{\boldsymbol{u}}\left(x, y, t_i\right) = \boldsymbol{v}^0\left(x, y\right), \ \ \forall\left(x, y\right) \in \Omega, \ t_i \in \left(0, T\right] \tag{10}$$

Equations (9) and (10) define the initial conditions where $\boldsymbol{u}^T = \left\{u, v, w\right\}$ e $\dot{\boldsymbol{u}}^T = \left\{\dot{u}, \dot{v}, \dot{w}\right\}$.

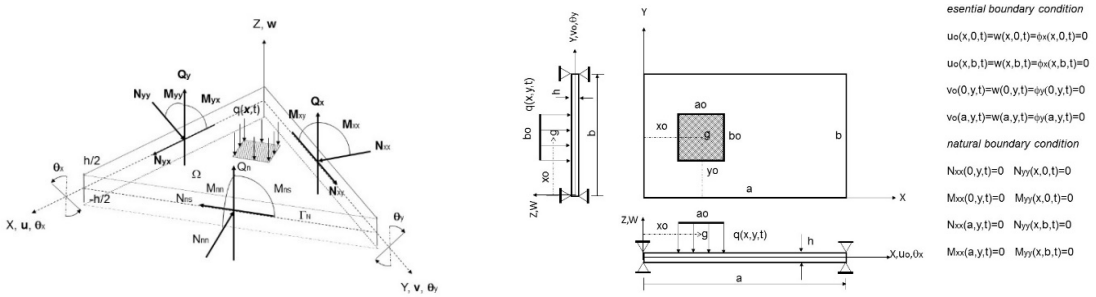

(a) (b)

Figure 1: a) internal and boundary forces in element plate; b) Simply supported plate with essential and natural boundary conditions and sectorial load.

2.3 Semi-discrete formulation for the problem of forced vibrations

The semi-discrete formulation is obtained for the theoretical example of homogeneous and isotropic plate presented by Fig. 1 (b) using the Bubnov-Galerkin method applied on the residue function obtained of the elastodynamics equilibrium equations.

The problem in question is to determine the vectors $\boldsymbol{u}_h\left(x, y, t\right)$, $\boldsymbol{\psi}_h\left(x, y, t\right)$, $w_h\left(x, y, t\right) \in \delta_h$ defined in equations (12) to (14) where:

$$\delta_h = \left\{\boldsymbol{u}_h, \boldsymbol{\psi}_h, w_h \in H^1\left(\bar{\Omega}\right) \times \left(0, T\right] \mid \boldsymbol{u}_h = \bar{\boldsymbol{u}}, \boldsymbol{\psi}_h = \bar{\boldsymbol{\psi}}, w_h = \bar{w}, \boldsymbol{x} \in \Gamma_D, \forall t \in \left(0, T\right]\right\}. \tag{11}$$

$$\boldsymbol{u}_h\left(x, y, t\right) = \begin{Bmatrix} u_o\left(x, y, t\right) \\ v_o\left(x, y, t\right) \end{Bmatrix}_h = \boldsymbol{N}^{(0)}\boldsymbol{U}(t) \tag{12}$$

$$\boldsymbol{\psi}_h\left(x, y, t\right) = \begin{Bmatrix} \theta_x\left(x, y, t\right) \\ \theta_y\left(x, y, t\right) \end{Bmatrix}_h = \boldsymbol{N}^{(1)}\boldsymbol{U}\left(t\right) \tag{13}$$

$$w_h\left(x, y, t\right) = \boldsymbol{N}^{(2)}\boldsymbol{U}\left(t\right). \tag{14}$$

In equations (12) to (14), $\boldsymbol{N}^{(m)}$, $m = 0, 1, 2$ and $\boldsymbol{U}\left(t\right)$ are the matrices of shape functions and the vector of displacement parameters described in equations (15) to (18).

$$\boldsymbol{N}^{(0)} = \begin{bmatrix} \cdots & H_i^j & 0 & 0 & 0 & 0 & \cdots \\ \cdots & 0 & H_i^j & 0 & 0 & 0 & \cdots \end{bmatrix} \tag{15}$$

$$\boldsymbol{N}^{(1)} = \begin{bmatrix} \cdots & 0 & 0 & H_i^j & 0 & 0 & \cdots \\ \cdots & 0 & 0 & 0 & H_i^j & 0 & \cdots \end{bmatrix} \tag{16}$$

$$\boldsymbol{N}^{(2)} = \begin{bmatrix} \cdots & 0 & 0 & 0 & 0 & H_i^j & \cdots \end{bmatrix} \tag{17}$$

$$\boldsymbol{U}^T = \begin{Bmatrix} \cdots & u_i^j(t) & v_i^j(t) & \theta_{xi}^j(t) & \theta_{yi}^j(t) & w_i^j(t) & \cdots \end{Bmatrix},\ i = 1,...,N_n,\ j = 1,...,(1+k)^2 \tag{18}$$

In equations (15) to (18) $H_i^j(x,y)$ are global functions, with regularity $C^k(\Omega),\ k = 1,2$, obtained with Hermite elements. In eq. (18), N_n is the number of nodes in the domain discretization grid and the supra-index *j* is the number of global functions per grid node. More details on obtaining the functions in Hermite elements are presented in [13]. The discrete formulations for the deformations are shown in equations (19) to (22).

$$\varepsilon^{(m)} = \boldsymbol{B}^{(m)}\boldsymbol{U}(t),\ m = 0,1. \tag{19}$$

$$\boldsymbol{B}^{(m)} = \boldsymbol{H}\boldsymbol{J}\boldsymbol{\partial}_\zeta \boldsymbol{N}^{(m)}. \tag{20}$$

In eq. (18) the operators $\boldsymbol{H}$, $\boldsymbol{J}$ and $\boldsymbol{\partial}_\zeta$ are shown in detail in Garcia and Rossi [15].

$$\varepsilon^{(2)} = \boldsymbol{B}^{(2)}\boldsymbol{U}(t) \tag{21}$$

$$\boldsymbol{B}^{(2)} = \boldsymbol{N}^{(1)} + J\partial_s \boldsymbol{N}^{(2)} \tag{22}$$

In eq. (22), $\boldsymbol{J}$ is the Jacobian matrix and ∂_s is the gradient operator for a vector both detailed in [15]. Discrete formulations for acceleration vector gradients $\ddot{\boldsymbol{u}}_h$, $\ddot{\boldsymbol{\psi}}_h$ and $\ddot{w}_h$, used in obtaining the non-local mass matrix, are shown in equations (23) to (26).

$$\nabla\left(\ddot{\boldsymbol{f}}_h^m\right) = \boldsymbol{G}^{(m)}\ddot{\boldsymbol{U}}(t). \tag{23}$$

$$\boldsymbol{G}^{(m)} = \boldsymbol{J}\boldsymbol{\partial}_\zeta \boldsymbol{N}^{(m)}. \tag{24}$$

$$\nabla\ddot{w}_h = \boldsymbol{G}^{(2)}\ddot{\boldsymbol{U}}(t). \tag{25}$$

$$\boldsymbol{G}^{(2)} = J\partial_s \boldsymbol{N}^{(2)}. \tag{26}$$

In eq. (23), $\ddot{\boldsymbol{f}}_h^0 = \ddot{\boldsymbol{u}}_h$ and $\ddot{\boldsymbol{f}}_h^1 = \ddot{\boldsymbol{\psi}}_h$.

The weak formulation defined by eq. (28) was obtained by the Galerkin method from the weighting of the residual function obtained from equations (3) to (8) and from the incorporation of discrete forms defined by equations (12) to (26) for the plate in Fig. 1(b) with zero natural boundary conditions. At eq. (28), $\boldsymbol{C}_n$, $\boldsymbol{C}_b$ and $\boldsymbol{C}_s$ are the matrices corresponding to normal forces and normal deformations, moments and curvatures and shear forces and shear deformations. The matrices $\boldsymbol{C}_n$ and $\boldsymbol{C}_b$ are shown in detail in [15], and $\boldsymbol{C}_n$ is defined by eq. (27). The terms λ_u, λ_b and λ_w are the penalty coefficients corresponding to the vectors $\boldsymbol{u}_h$, $\boldsymbol{\psi}_h$ and w_h.

$$\boldsymbol{C}_n = \frac{1}{h^2}\boldsymbol{C}_b \tag{27}$$

At eq. (28) the terms in parentheses that multiply the parameter vector $\boldsymbol{U}(t)$ represent the stiffness matrix $\boldsymbol{K}$, the terms that multiply the vector of acceleration parameters $\ddot{\boldsymbol{U}}(t)$ represent the mass matrices of classical elasticity and non-local elasticity.

$$\left(\int_{\Omega} \boldsymbol{B}^{(0)T} \boldsymbol{C}_n \boldsymbol{B}^{(0)} d\Omega + \int_{\Omega} \boldsymbol{B}^{(1)T} \boldsymbol{C}_b \boldsymbol{B}^{(1)} d\Omega + \int_{\Omega} \boldsymbol{B}^{(2)T} \boldsymbol{C}_s \boldsymbol{B}^{(2)} d\Omega \right.$$

$$\left. + \int_{\Gamma_D} \lambda_u \boldsymbol{N}^{(0)T} \boldsymbol{N}^{(0)} d\Gamma + \int_{\Gamma_D} \lambda_b \boldsymbol{N}^{(1)T} \boldsymbol{N}^{(1)} d\Gamma + \int_{\Gamma_D} \lambda_s \boldsymbol{N}^{(2)T} \boldsymbol{N}^{(2)} d\Gamma \right) \boldsymbol{U}\left(t\right) + \int_{\Omega} \boldsymbol{N}_w^T q d\Omega - \int_{\Omega} \mu \nabla^2 q \boldsymbol{N}_w^T d\Omega$$

$$+ \left(\int_{\Omega} I_0 \boldsymbol{N}^{(0)T} \boldsymbol{N}^{(0)} d\Omega + \int_{\Omega} I_2 \boldsymbol{N}^{(1)T} \boldsymbol{N}^{(1)} d\Omega + \int_{\Omega} I_0 \boldsymbol{N}^{(2)T} \boldsymbol{N}^{(2)} d\Omega \right) \ddot{\boldsymbol{U}}\left(t\right)$$

$$+ \left(\int_{\Omega} I_0 \mu \boldsymbol{G}^{(0)T} \boldsymbol{G}^{(0)} d\Omega + \int_{\Omega} I_2 \mu \boldsymbol{G}^{(1)T} \boldsymbol{G}^{(1)} d\Omega + \int_{\Omega} I_0 \mu \boldsymbol{G}^{(2)T} \boldsymbol{G}^{(2)} d\Omega \right) \ddot{\boldsymbol{U}}\left(t\right) = 0 \tag{28}$$

Yet in eq. (28) the integrals associated with external forces in the domain constitute the vector $\boldsymbol{F}(t)$. In this way the elastodynamic equation represented by eq. (28) can be shown in matrix form by eq. (29).

$$\left(\boldsymbol{M}_l + \boldsymbol{M}_{nl}\right)\ddot{\boldsymbol{U}}\left(t\right) + \boldsymbol{K}\boldsymbol{U}(t) = \boldsymbol{F}(t)\,. \tag{29}$$

3 Numerical Result

The results of free and forced vibrations are obtained for moderate thick graphene plates with load and boundary conditions shown in Fig.1 (b). For the two examples analyzed in this section, the plates are constituted of homogeneous and isotropic material with modulus of elasticity of $E = 1TPa$, Poisson's ratio of $\nu = 0.16$ and mass density of $\rho = 2250\,kg\,/\,m^3$. In the study, the penalty coefficients are considered $\lambda_u = \lambda_b = \lambda_w = 1 \times 10^{15}$. The numerical strategies used are defined in Tab.1.

Table 1. Numeric model

strategy	element type	grid	NDOF
A	HFEM C[1]	10×10	2420
B	HFEM C[2]	8×8	3645

3.1 Free vibrations

In this study the influence on the first natural frequency of the increase of dimensions in the plane $\left(x, y\right)$ on a square plate with thickness $h = 0.34nm$ and the nanoscale coefficient $\mu = 1,41\left(nm^2\right)$. The results are analyzed using the nominal values and the relative error of the first natural frequency in relation to the DM (reference values) defined in eq. (30). The results obtained with the numerical model in the Tab.1 are compared with the Generalized Differential Quadrature Method (GQDM) cited in [8] and shown in the Figures 2(a) and 2(b).

$$e_r = \left|\omega_h^1 - \omega_D^1\right| \Big/ \left|\omega_D^1\right| \tag{30}$$

In eq. (28), ω_h^1 and ω_D^1, are the results for the first natural frequency obtained by the numerical models in Tab.1 and by the reference values obtained with MD respectively. The Figures (2a) and (2b) show that for $a = b > 10nm$ the results obtained with the proposed strategies are closer to those obtained by MD than by GDQM. The results obtained corroborate the principles of non-local elasticity where, with increasing dimensions, the results tend towards those obtained with classical elasticity.

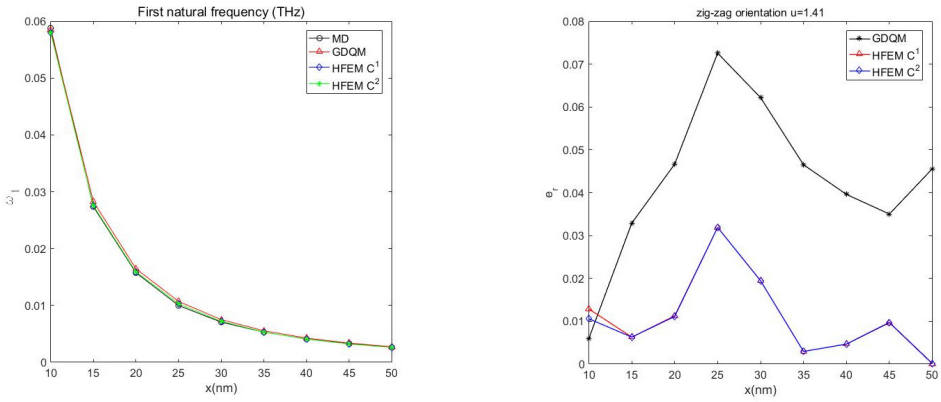

(a) (b)

Figure 2: a) First natural frequency for μ=1,41nm²; b) relative error vs. plate dimensions

3.2 Forced vibrations

In this study, the phenomenon of wave dispersion that occurs with the variation of nano scale coefficients and plate dimensions is analyzed. The results are analyzed by the propagation of the mechanical wave of the component $w\left(a/2, a/2, t\right)$ for a simply supported plate shown in Fig. 1(b). The dispersion phenomenon is analyzed by the amplitude and wavelength for plates with dimensions $a = b = \left\{10, 30\right\}\left(nm\right)$, ratio $a/h = 10$ and for coefficients $\mu = \left\{0, 1, 2, 4\right\}\left(nm^2\right)$. The excitation force is evenly distributed with rations $a/a_o = b/b_o = 1$ according Fig.1(b) and produced by the harmonic signal shown in eq. (28).

$$\boldsymbol{F}(t) = \boldsymbol{q} sen\left(2\pi\omega t\right) \tag{28}$$

In eq. (20), $\omega = 0.2\,THz$ e $\boldsymbol{q}^T = \left\{0, 0, 0, 0, 10^6\right\} Pa$. The results are analyzed for the strategies A and B mentioned in Tab.1 and are compared with a semi-analytical solution of classic elasticity. This solution is obtained using the semi-discrete formulation of eq. (26) and the bi-harmonic modes used to approach the problem of FSDT plates as shown in [14]. The results in this study, shown in Fig. 3(a), show the significant influence of mechanical wave dispersion for the plate with dimensions 10 nm x10 nm when the nanoscale coefficient is increased. On the other hand, with the plate dimensions increasing to 30 nm x30 nm, the dispersion effect is reduced, as shown in Fig. 3 (b), the propagation phenomenon being less sensitive to the effects of the variation of the nanoscale coefficients. In this case, again with the increase in the dimensions of the plate, the dispersion results are not very sensitive to the variation of the nanoscale coefficients and converge to those obtained with the classic elasticity.

4 Conclusion

The comparative results for the first natural frequency showed results very close to those obtained with molecular dynamics for the numerical strategies proposed in this work. In the study of the phenomenon of propagation of mechanical waves the results of the proposed strategies were satisfactory when compared to the classic version of elastodynamics obtained with $\mu = 0$. The wave dispersion phenomena resulting from variations in dimensions and nanoscale coefficients were adequately represented by the proposed numerical models.

Acknowledgements. The authors of this work would like to thank CAPES for financial support through the postdoctoral scholarship and the infrastructure provided by UFRGS. Also, to the CNPq and FAPERGS for financial research support. Grant numbers: CNPq 306058/2018-9, FAPERGS: 19/2551-0001954-8-1.

Authorship statement. The authors confirm that they are solely responsible for the authorship of this work, and that all material that has been included here as part of this paper is either owned (and authored) by the authors or has the permission of the owners to be included here.

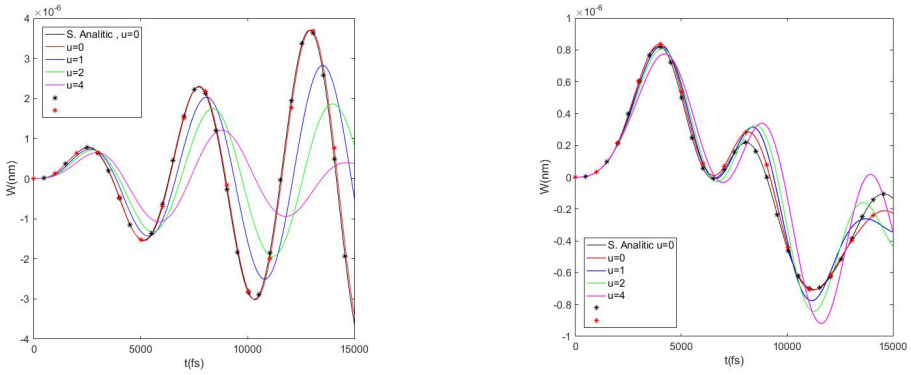

(a) (b)

Figure 3: Wave propagation for the displacement component w (a/2, a/2, t); a) plate of 10 nm x10 nm; b) plate of 30 nm x30 nm.

References

[1] Nao Y. and Vicenzo L. "Young's Modulus of single walled carbon nanotube". *Journal of Applied Phisics*, vol. 84, n. 4, 1998.

[2] A. Moisala, Q. Li, I.A. Kinloch, A.H. Windle. "Thermal and electrical conductivity of single and multi-walled carbon nanotube-epoxi composite". *Composites Science and Technology*, vol. 66, pp 1285-1288, 2006.

[3] D. Garcia-Sanchez, A. San Paulo, M. J. Esplandiu, F. Perez-Murano, L. Forro´, A. Aguasca, and A. Bachtold. "Mechanical detection of carbon nanotube resonator vibration". *Phisical Review Letters*, vol. 99, n. 085501, 2007.

[4] S.C. Chowdhury, T. Okabe. "Computer simulation of carbon nanotube pull-out from polymer by the molecular dynamics method". *Composites: Part A,* vol. 38, pp 747–754, 2007.

[5] Daniel Sanchez-Portal, Emilio Artacho, and Jose´ M. Soler. "*Ab initio* structural, elastic, and vibrational properties of carbon nanotubes". *Physical Review B*, vol. 59, n. 19, 1999.

[6] A. C. Eringen. "Theory of micromorphic materials of with memory". *International Journal of Engineering and Science*, vol. 10, pp 623-641, 1972.

[7] A. C. Eringen. "On differential equations of nonlocal elasticity and solutions of screw dislocation and surface waves". *Journal of Applied Physic*, vol. 54, n. 4703, 1983.

[8] R. Ansari, S. Sahmani, B. Arash. "Nonlocal plate model for free vibrations of single-layered graphene sheets". *Physics Letters A*, vol. 375, pp 53–62, 2010.

[9] L.W. Zhang, Yang Zhang, K.M. Liew. "Vibration analysis of quadrilateral graphene sheets subjected to an inplane magnetic field based on nonlocal elasticity theory". *Composites Part B*, vol. 118, pp 96-103, 2017.

[10] B. Arash, Q. Wang, K.M. Liew. "Wave propagation in graphene sheets with nonlocal elastic theory via finite element formulation". *Computer Method in Applied Mechanic and Engineering*, vol. 223-224, pp 1-9, 2012.

[11] Tolga Aksencer, Metin Aydogdu. "Forced transverse vibration of nanoplates using nonlocal elasticity". *Physica E*, vol. 44, pp 1752–1759, 2012.

[12] Mohammad Reza Barati and Hossein Shahverdi. "Forced vibration of porous functionally graded nano plates under uniform dynamic load using general nonlocal stress-strain gradient theory". *Journal of Vibration and Control*, pp 1-16, 2017.

[13] R. Mazzochi. Elementos finitos quadrilaterais hermitianos de alta regularidade gerados pela partição de unidade aplicados na solução de problemas de elasticidade e elastodinâmica. Msc. Thesis, Universidade Federal do Rio Grande do Sul, 2014.

[14] J. N. Reddy. "Mechanics of laminated composite plates and shells theory and analysis". CRC Press LLC, 2004.

[15] O. A. Garcia., R. Rossi. "A G/XFEM approximation space based on the enrichment of rational polynomials to model free and forced vibration in elastic isotropic Mindlin-Reissner Plates". *Journal of the Brazilian Society of Mechanical Sciences and Engineering*, 41:134, 2019.